ISSN 2321-807X
Volume 12 Number20
Journal of Advances in chemistry

Prediction of Stability and Thermal conductivity of MgO Nanofluids using CCRD Statistical Design Analysis

P.Pandiyaraj, A.Gnanavelbabu, P.Saravanan
Research Scholar, Dept. of Mechanical Engg, CEG Anna University Chennai
Pandia2000@gmail.com
Associate Professor, Dept. of Industrial Engg, CEG Anna University Chennai
agbabu@annauniv.edu
Research Scholar, Dept. of Industrial Engg, CEG Anna University Chennai
assarankings@gmail.com

ABSTRACT

Magnesium oxide nanopowders were synthesized by chemical reduction method in which sodium hydroxide solution was used as a reducing agent. Magnesium nitrate ($MgNO_3.6H_2O$) precursor was used for the synthesis of MgO nanopowders. Solid state characterizations of synthesized nanopowders were carried out by infrared spectroscopy (FTIR) and X-ray diffraction (XRD) techniques. Using two step method, synthesized nanopowders were prepared as nanofluids by adding water and ethylene glycol (55:45). Thermal conductivity measurements of prepared nanofluids were studied using transient hot wire apparatus in which maximum thermal conductivity enhancement was observed in nanofluid. CCRD design has been applied to optimize the performance of nanofluid systems. In this regard, the performance was evaluated by measuring the stability and thermal conductivity ratio based on the critical independent variables such as temperature, particle volume fraction and the pH of the solution. A total of 20 experiments were accomplished for the construction of second-order polynomial equations for both target outputs. All the influential factors, their mutual effects and their quadratic terms were statistically validated by analysis of variance (ANOVA). The optimum stability and thermal conductivity of MgO nanofluids with various temperature, volume fraction and particle fraction were studied and compared with experimental reults. The results revealed that, at increase in particle concentration and pH of nanofluids at certain point would increase thermal conductivity and become stable at nominal temperature. According to the results, the predicted values were in reasonable agreement with the experimental data as more than 95% of the variation could be predicted by the CCRD model for thermal conductivity ratio and zeta potential.

Indexing terms/Keywords

MgO nanofluid, Thermal conductivity, Zeta Potential, CCRD

Academic Discipline And Sub-Disciplines

Nanotechnology and Nanofluids

SUBJECT CLASSIFICATION

Enhancement of Thermal conductivity and Zeta Potential

TYPE (METHOD/APPROACH)

Experimental analysis of MgO nanofluids using two step method and statistical analysis of MgO Nano fluids for Thermal conductivity and zeta potential using CCRD design.

INTRODUCTION

Magnesium oxide (MgO) is a versatile oxide material, with high melting point (2850 ºC) and high boiling point (3600 ºC); thereby it is thermally so stable. In bulk, to make pure MgO, one of the methods is burning magnesium ribbon in the presence pure oxygen, but metallic magnesium is considerably expensive. Due to its high melting point, magnesium oxide possesses inflexible properties, so it can be used as a body material, furnace and crucibles. MgO compounds were prepared by those conventional methods often yields a relative small surface area and hence shows low reaction activity [1]. It has been reported that the catalytic properties of sol-gel MgO catalyst strongly depend on the crystallite size, surface area, structure defects and acid-basic concentration. In nano scale, to synthesize MgO nanoparticles, wet chemical and sol gel techniques are followed with suitable reducing agent and further treated to annealing process [9]. Recently, sol-gel process has assumed a special significance for synthesis MgO compounds because it is simple, cost effective, and capable of yielding unique properties such as large surface area-to-volume ratio and narrow particle size distribution at relative low temperatures [2]. It is believed that the materials prepared by the sol-gel technique show much better surface of bulk properties than those obtained from the conventional methods. Several factors such as annealing temperature, annealing time, pH, catalytic agents and environment conditions drastically affect the characteristics of the magnesium oxides [3]. Higher densification of chips leads to more heat dissipation. Most electronic devices face thermal management challenges and the reduction of existing surface area for heat elimination. So, the reliable thermal management system is much needed to overcome this problem. Nanofluids with higher thermal conductivities are established convective heat transfer coefficients than the base fluids. Those nanofluids were inside the flat plate heat pipes as a working fluid. Nanofluids inside the flat plate heat pipes reduce the thermal resistance considerably high. And also nanofluids reduce the temperature difference between the heated wick and the coolant. A combined heat wick with nanofluids had the efficiency

to eliminate high heat flux of upcoming advanced electronic devices. Recent researches demonstrated that nanofluids could raise the heat transfer coefficient by increasing its thermal conductivity. Conventional heat transfer fluids like water, ethylene glycol, metallic fluids were widely used in the past decade as a working fluid [4]. But they lacks in enhancement of thermal properties because of their suspension property under the range of micro-sized particles. Sedimentation of those micro-sized particles from suspension causes clogging channels due to poor stability and rheological properties. The thermal resistance of heat pipes depends on the thermal characteristics of working fluids. The better thermal characteristics of working fluids are more important to refining the thermal performance of heat pipes. Hence the nanofluids from nanoparticles have been preferred over conventional heat transfer fluids because of its thermal stability and non-settlement under fixed conditions over a weeks or months [5]. The nanofluids produce enhanced heat transfer rate compared to normal fluids [6]. The heat transfer rate of working nanofluid depends upon three major factors such as thermal conductivity, heat capacity and viscosity. The thermal conductivity of the nanofluids increases with temperature but thermal conductivity models are failed to predict the thermal conductivity of nanofluids [7]. The enhanced thermal conductivity of the CuO nano fluids dispersed in water/ethylene glycol was investigated which concluded that the thermal conductivity of nanofluids depends on particle size and shape of nanoparticles [8]. Viscosity and particle concentration significantly increases the thermal conductivity of Al_2O_3 nanoparticles [9]. Low nanoparticle concentration leads to Newtonian behavior in ZnO-EG nanofluids which considerably affects the thermal conductivity [10]. The friction factor of nanoparticles at low concentration produces negligible penalty in pumping consumption. Nearly 20% of penalty in pressure drop increases 25% of heat transfer coefficient. Dynamic viscosity of MgO-water based nanofluids enhanced the heat transfer performance and thermo physical properties of the nanofluids [11]. Recently a Researcher used fractional full factorial design in order to determine the significant influence of different factors like temperature, particle concentration, pH of the nanofluid, density of the nanoparticles, sonication duration [12]. The thermophysical properties of nanofluid needs water, ethylene glycol and oil as base fluid which was a popular research in the area of nanofluids. Conversely, very few papers are available on magnesium oxide based nanofluids. MgO nanofluid has good chemical and physical stability which wide up the investigation among the researchers considerably. Therefore in the current research, MgO/EG–water (40–60%) was prepared in binary mixture of water/ethylene glycol and its thermal conductivity was measured experimentally. Literature survey reveals that there are no works on the prediction of thermal conductivity of the nanoparticles dispersed in binary mixture of water and ethylene using statistical design approach. Moreover, there is no appropriate statistical model to prepare and estimate the thermal conductivity of the nanofluid, hence innovative correlations in terms of temperature, particle concentration (volume fraction), pH using CCRD design have been suggested and compared with obtained experimental data.

EXPERIMENTAL ANALYSIS:

Synthesis of MgO nanoparticle:

Reagents such as, Magnesium nitrate ($MgNO_3.6H_2O$), Sodium hydroxide (NaOH) and other chemicals are used in the synthesis of MgO nanoparticles. De-ionized water was prepared in the laboratory to be used as solvent. Magnesium oxide nanoparticles were synthesized by magnesium nitrate ($MgNO_3.6H_2O$) as a precursor and sodium hydroxide as reducing agent. At first, 0.2M magnesium nitrate ($MgNO_3.6H_2O$) was completely dissolved with sonification in 100 ml of double distilled water and stirred well for 30 minutes. Then 0.5M sodium hydroxide was dissolved in 100 ml of double distilled water and stirred well for 30 minutes. Now prepared reducing agent (NaOH) is added drop wise in the existing magnesium nitrate ($MgNO_3.6H_2O$) solution, and stirred continuously. Later white precipitation of magnesium hydroxide is formed. The stirring was continued for 30 minutes. The precipitate was cleaned with filtration and thoroughly washed with methanol to remove ionic impurities and then the powder samples were annealed in atmospheric air for more than two hours at 200º and 400º C. The preparation chart of MgO nanoparticles is shown in Fig 1.

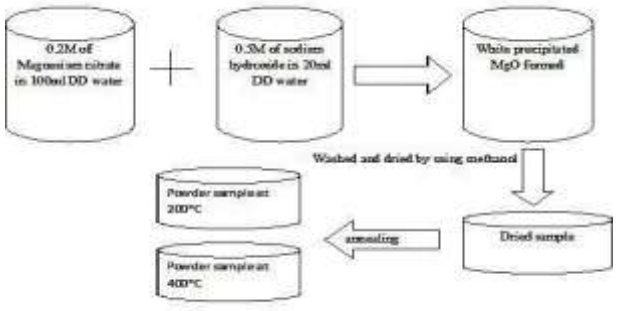

Fig 1: Preparation Chart of MgO Nanoparticles

To confirm the presence of Magnesium oxide nanoparticles, UV-Visible spectroscopy (JASCO V 650) characterization has been done. The crystallinity and crystal phases are determined by X-ray powder diffraction (XRD). Then the synthesized magnesium oxide nanoparticle was also analyzed using the Fourier transform infrared spectroscopy (FT-IR).

Preparation of MgO nanofluid:

For the preparation of MgO nanofluids, 50 mg magnesium oxide nano powder was mixed with 50 mL of ethylene glycol/water base fluid (45:55 volume media) and stirring for 2 h. In the resulting solution 0.1% poly vinyl pyrrolidone (PVP) (50mg) and 1.0% sodium laurel sulfate (SLS) (500mg) were mixed with continuous stirring for 3 h. For proper dispersion the resulting solutions were kept on sonicator for 2 h. The pH was organized by hydrochloric acid (HCl) and sodium hydroxide (NaOH).

UV spectroscopy:

Magnesium oxide nanoparticles were prepared by electrochemical route using sol-gel method at room temperature and analysed by UV-Visible spectroscopy (JASCO V 650). Fig 2 represents the optical absorption spectra of Magnesium oxide respectively. The characteristic SPR symmetric of 300nm with an absorbance of 0.9 obtained for red colour magnesium oxide nanoparticles.

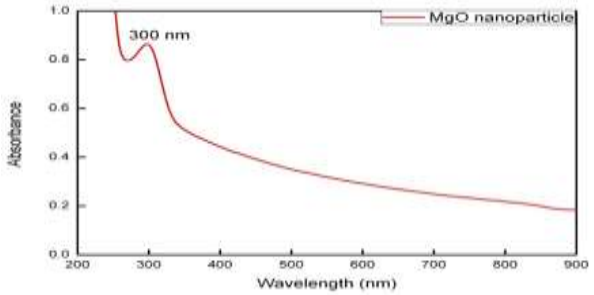

Fig 2: UV Spectroscopy of MgO

FT-IR Analysis:

The FT-IR spectra of MgO taken after the synthesis of nanoparticles at 200^{0}C and 400^{0}C were analyzed for the determination of possible functional groups which leads to formation of metal nanoparticles. The FTIR spectrum for the annealed MgO nano powder is shown in Fig 3. From FT-IR results, the stretching vibration mode for the Mg–O–Mg compound was in the range of 433–575 cm^{-1} as a broad band. Two different bands are found at the wave number ranges of 1122–1208 cm^{-1} and 1388–1462 cm^{-1} and they are recognized to the bending vibration of completely absorbed water molecule and surface hydroxyl group (–OH), correspondingly.

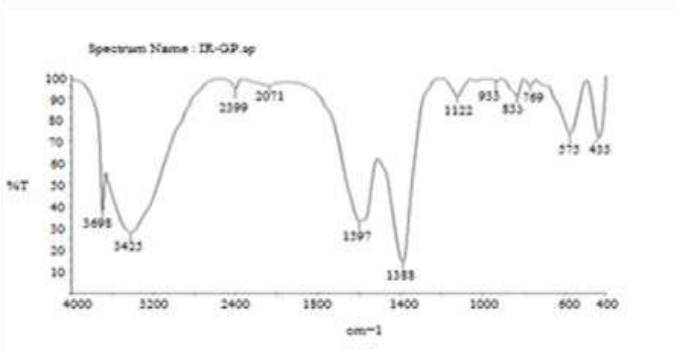

Fig 3: FTIR Graph of Annealed MgO

A unique broad vibration band was found in the wavenumber range 3425– 3698 cm^{-1} because of O–H stretching vibration of aerial absorbed water molecule and surface hydroxyl group. The FT-IR absorption peak was found at the wavenumber 1493 cm^{-1}, it allots the asymmetric stretching of the carbonate ion .

TGA/DTA:

Thermal decomposition behavior of the Annealed MgO was investigated using TGA/DTA. The weight loss occurred till 680°C for the MgO. The exothermic peak is observed at 607ºC. The organic residues are disappeared at a temperature 567.25°C and 586.37ºC. From the TGA/DTA curve, the complete weight loss is observed at 676.48°C which is shown in fig 4.

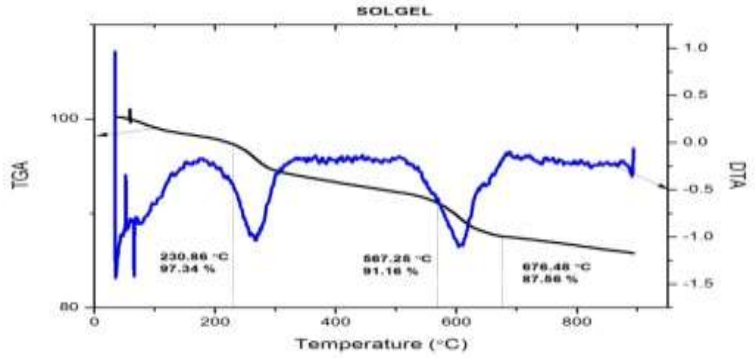

Fig 4: TGA/DTA Analysis of Annealed MgO

X-Ray Diffraction:

The powder XRD was set in the 2θ range between 20° to 80° using Cu Kα radiation. The powder XRD patterns were taken for both MgO nanoparticles as before annealed and after annealed. From these XRD patterns on Fig 5, we found that the annealed material was crystallized and occurs in solitary phase under cubic symmetry. The Bragg reflection Peaks of (111), (002), (202), (113), and (222) are seen in the 2θ range between 20 and 80°. Reflections are so sharp and broadening slightly. Those reflections confirm the crystalline nature of MgO nanopowder. By using the Debye Scherrer formula, the average crystalline size around 22-23 is obtained for annealed MgO nano powder from XRD powder data.

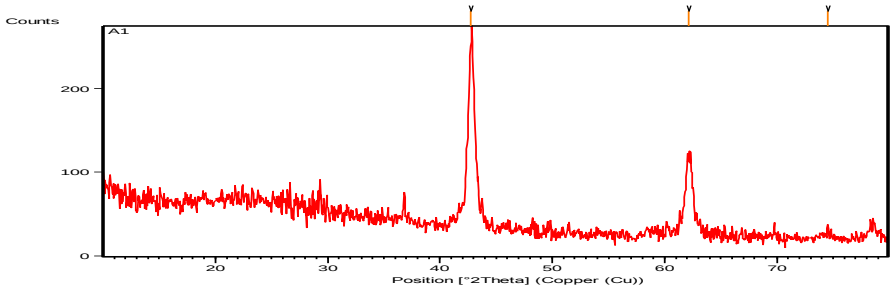

Fig 5: XRD of Annealed MgO

THEORETICAL ANALYSIS

Response Surface Methodology (RSM)

To minimize the experimental runs in manufacturing arena, designing experiments using statistical techniques were used. Among the various methods of designing experiments, response surface methodology (RSM) is a combination of mathematical and statistical techniques that are useful for modeling and analyzing the influence of several design variables on the response and the objective is to optimize this response [13]. For each independent factor, the quadratic coefficients in the second-order model may be evaluated by applying 3 levels. When independent factors increases in 3^n factorial design, the number of obligatory runs quickly increases as per statistical approach. But sometimes, this may lead to more time duration for more number of experimental runs and turns costly too. Hence here we selected the sequential design called central composite design (CCD) which reduces the number of experiments than the 2-level full factorial design. So, 2n points of the full factorial 2-level design were combined with center point recurrence of nominal design and 2n axial runs to produce a CCD. By the way, in this research, RSM based on the CCD has been applied for the modeling of the nanofluid system using Design Expert version 8.0.7.1 statistical software (Stat-Ease Inc.). Three independent design variables as temperature (X_1), particle concentration (X_2) and pH (X_3) were investigated with the actual and coded values shown in Table 1.

Table 1 Design Variables for CCD

Independent variables	Symbol	Coded and actual variable level				
		Star-low	Low	Center	High	Star-high
		-1.68	-1	0	1	1.68

Temperature (ºC)	X_1	20	30	45	60	70
Particle Concentration (%vol)	X_2	0.66	1	1.50	2	2.34
Solution pH	X_3	4.6	6	8	10	11.4

For the three factors, CCRD with a quadratic model is composed of the full 23 factors with its 8 cubic points, augmented with six replications of the center points and the six axial (star) points. Rotatable design makes the variance of prediction depend only on the scaled distance of the center of the design [14]. Central composite designs with different properties can be developed by taking different α values. To make the design rotatable, the axial distance α was assigned a value of 1.68.

Measurement of the Stability and Thermal Conductivity of the Nanofluid

Thermal conductivity measurements were performed by a Transient Hot Wire technique, which is a perfect method for determining the thermal conductivity of fluids [15]. A THW system uses a platinum wire suspended symmetrically inside a fluid which placed inside a vertical cylindrical container. Nagasaka and Nagashima's method, in which the wire is coated with a thin electrical insulation layer, was used in the research experiment to eliminate error and measurement of electrically conducting fluids [16]. Generally, the Transient hot wire technique works under the principle of measuring the temperature/time response of the wire to an electrical pulse. The wire is used as heater element and also as thermometer, thereby thermal conductivity, k is calculated from a derivation of Fourier's Law where q is the applied electric power and T_1 and T_2 are the temperatures at times t_1 and t_2.

$$k = \frac{q}{4\pi(T_2 - T_1)} \ln \frac{t_2}{t_1}$$

The temperature coefficient of the wire's resistance reveals the temperature rise of the wire. Therefore the temperature rise of the wire can be determined by the change in its electrical resistance with respect to time. Regulation experiments were performed for MgO inside water/ethylene glycol in the temperature range of 250-300 K and at atmospheric pressure. Investigations show that heaping of particles and accumulation are the key skins in the stability and enhancement of the thermal conductivity of nanofluids [17]. Hence, we prepared a highly homogenized and aggregated nanofluid to have better stability and thermal conductivity. A stable suspension requires a good dispersion of the small particle in the liquid medium and a higher absolute value of the zeta potential of the particles [18]. Then, zeta potential was measured by a Malvern Nano-ZS (Malvern Instrument Inc., London, UK).

RESULTS AND DISCUSSIONS

Design of the Experiments and Response Surface Modeling

According to a CCD configuration and design, 20 different combination conducts were carried out in random order and the responses of zeta potential (mV) and the thermal conductivity ratio were determined experimentally and predicted by the fit model. The results are summarized in Table 2.

Table 2 Design layout and experimental results of the CCRD

Std	Run	Block	A	B	C	Thermal Conductivity		Zeta Potential	
						Experimental	Predicted	Experimental	Predicted
1	3	Block 1	-1.00	-1.00	-1.00	0.83	0.84	-21	-22.26
2	7	Block 1	1.00	-1.00	-1.00	0.91	0.91	-29	-30.66
3	16	Block 1	-1.00	1.00	-1.00	0.87	0.87	-27	-27.64
4	18	Block 1	1.00	1.00	-1.00	0.95	0.95	-33	-33.03
5	9	Block 1	-1.00	-1.00	1.00	0.85	0.86	-25	-25.93

6	14	Block 1	1.00	-1.00	1.00	0.92	0.93	-36	-36.32
7	5	Block 1	-1.00	1.00	1.00	0.89	0.90	-31	-30.30
8	15	Block 1	1.00	1.00	1.00	0.99	0.99	-38	-37.70
9	11	Block 1	-1.68	0.00	0.00	0.84	0.83	-29	-28.19
10	19	Block 1	1.68	0.00	0.00	0.97	0.97	-42	-41.45
11	20	Block 1	0.00	-1.68	0.00	0.93	0.92	-32	-29.98
12	10	Block 1	0.00	1.68	0.00	0.98	0.98	-35	-35.66
13	17	Block 1	0.00	0.00	-1.68	0.86	0.85	-23	-21.32
14	12	Block 1	0.00	0.00	1.68	0.9	0.89	-28	-28.32
15	6	Block 1	0.00	0.00	0.00	0.94	0.94	-37	-36.21
16	8	Block 1	0.00	0.00	0.00	0.92	0.94	-36	-36.21
17	2	Block 1	0.00	0.00	0.00	0.96	0.94	-37	-36.21
18	1	Block 1	0.00	0.00	0.00	0.93	0.94	-34	-36.21
19	4	Block 1	0.00	0.00	0.00	0.95	0.94	-37	-36.21
20	13	Block 1	0.00	0.00	0.00	0.94	0.94	-36	-36.21

A second-order polynomial equation was used to find the mathematical relationship between the dependent variables (zeta potential and thermal conductivity ratio) and the set of independent variables. For three factors, the obtained model was expressed as follows:

$$y = b_0 + \sum_{i=1}^{n} b_i X_i + \sum_{i=1}^{n} b_{ii} X_{ii}^2 + \sum_{i<j} \sum_{j}^{n} b_{ij} X_i X_j$$

where y represents the predicted responses, X_i and X_j are the coded values of the independent variables, b_0 is the regression term at the center point, bi are the linear coefficients (main effect), bii are the quadratic coefficients and b_{ij} are the two-factor interaction coefficients. Also, for statistical calculation based on CCD, the relation between the dimensionless coded values of the independent variables (X_i) and the actual values of them (X_i) are defined as:

$$x_i = \frac{X_i - (X_{i,low} + X_{i,high})/2}{(X_{i,low} - X_{i,high})/2}$$

where $X_{i,high}$ and $X_{i,low}$ are the real values of the independent variables at high and low levels, respectively.

Analysis of Variance (ANOVA)

The ANOVA values for the RSM model obtained from CCRD was quadratic regression model which is used in the optimization of stability of thermal conductivity; which are respectively tabulated in Tables 3 and 4.

Table 3 Model Fit summary for Thermal Conductivity ratio response

SOURCE	**Sum of Squares**	**df**	**Mean of Squares**	**F Value**	**P value prob>F**	**Suggested**
Quadratic	0.011	3	3.574E-003	20.53	0.0001	

Table 4 ANOVA for Thermal Conductivity ratio response

SOURCE	**Sum of Squares**	**df**	**Mean of Squares**	**F Value**	**P value prob>F**	
Model	0.040	9	4.479E-003	25.73	< 0.0001	**significant**
A-Temperature	2.739E-003	1	2.739E-003	15.74	0.0027	
B-Particle Concentration	2.139E-004	1	2.139E-004	1.23	0.2936	
C-pH	3.228E-004	1	3.228E-004	1.85	0.2032	

AB	1.125E-004	1	1.125E-004	0.65	0.4401	
AC	1.250E-005	1	1.250E-005	0.072	0.7942	
BC	1.125E-004	1	1.125E-004	0.65	0.4401	
A^2	3.064E-003	1	3.064E-003	17.60	0.0018	
B^2	1.391E-004	1	1.391E-004	0.80	0.3925	
C^2	7.908E-003	1	7.908E-003	45.43	< 0.0001	
Residual	1.741E-003	10	1.741E-004			
Lack of Fit	7.408E-004	5	1.482E-004	0.74	0.6250	
Pure Error	1.000E-003	5	2.000E-004			
Cor Total	0.042	19				
Std. Dev.	0.013	R-Squared	0.9586			
Mean	0.92	Adj R-Squared	0.9214			
C.V. %	1.44	Pred R-Squared	0.8282			
PRESS	7.226E-003	Adeq Precision	16.542			

The Model F-value of 25.73 implies the model is significant. There is only a 0.01% chance that a "Model F-Value" this large could occur due to noise. Values of "Prob > F" less than 0.0500 indicate model terms are significant. In this case A, A^2, C^2 are significant model terms. Values greater than 0.1000 indicate the model terms are not significant. If there are many insignificant model terms (not counting those required to support hierarchy), model reduction may improve your model. The "Lack of Fit F-value" of 0.74 implies the Lack of Fit is not significant relative to the pure error. There is a 62.50% chance that a "Lack of Fit F-value" this large could occur due to noise. The "Pred R-Squared" of 0.8282 is in reasonable agreement with the "Adj R Squared" of 0.9214. "Adeq Precision" measures the signal to noise ratio. A ratio greater than 4 is desirable. The ratio of 16.542 indicates an adequate signal.

The ANOVA values for the RSM model obtained from CCRD was quadratic regression model which is used in the optimization of stability of Zeta Potential; which are respectively tabulated in Tables 5 and 6.

Table 5 Model Fit summary for Zeta potential ratio response

SOURCE	**Sum of Squares**	**df**	**Mean of Squares**	**F Value**	**P value prob>F**	**Suggested**
Quadratic	243.23	3	81.08	37.69	< 0.0001	

Table 6 ANOVA for Zeta Potential response

SOURCE	**Sum of Squares**	**df**	**Mean of Squares**	**F Value**	**P value prob>F**	
Model	560.69	9	62.30	28.96	< 0.0001	**significant**
A-Temperature	2.59	1	2.59	1.21	0.2979	
B-Particle Concentration	6.46	1	6.46	3.00	0.1138	
C-pH	6.09	1	6.09	2.83	0.1232	
AB	4.50	1	4.50	2.09	0.1787	
AC	2.00	1	2.00	0.93	0.3577	
BC	0.50	1	0.50	0.23	0.6401	
A^2	3.47	1	3.47	1.61	0.2326	
B^2	20.70	1	20.70	9.62	0.0112	
C^2	233.86	1	233.86	108.72	< 0.0001	
Residual	21.51	10	2.15			

Lack of Fit	14.68	5	2.94	2.15	0.2106	
Pure Error	6.83	5	1.37			
Cor Total	582.20	19				
Std. Dev.	1.47	R-Squared	0.9631			
Mean	-32.30	Adj R-Squared	0.9298			
C.V. %	4.54	Pred R-Squared	0.7907			
PRESS	121.85	Adeq Precision	19.407			

The Model F-value of 28.96 implies the model is significant. There is only a 0.01% chance that a "Model F-Value" this large could occur due to noise. Values of "Prob > F" less than 0.0500 indicate model terms are significant. In this case B^2, C^2 are significant model terms. Values greater than 0.1000 indicate the model terms are not significant. If there are many insignificant model terms (not counting those required to support hierarchy), model reduction may improve your model. The "Lack of Fit F-value" of 2.15 implies the Lack of Fit is not significant relative to the pure error. There is a 21.06% chance that a "Lack of Fit F-value" this large could occur due to noise. The "Pred R-Squared" of 0.7907 is in reasonable agreement with the "Adj R-Squared" of 0.9298. "Adeq Precision" measures the signal to noise ratio. A ratio greater than 4 is desirable. The ratio of 19.407 indicates an adequate signal. Statistical plots such as the actual versus predicted responses for different independent variables shows the independent distribution in a completely randomized design in figure 6. Therefore, the models are seems to be correct, because actual assumptions are satisfying with predicted ones and no possible outliers for both responses.

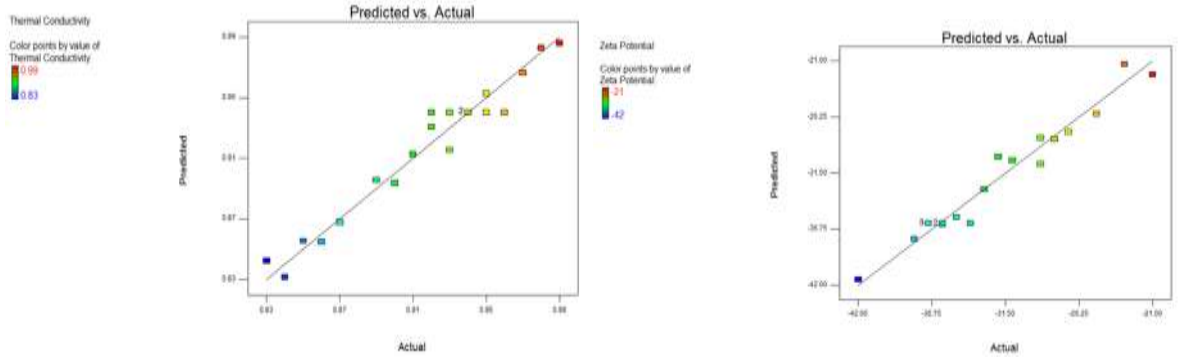

(a) (b)

Fig 6: Plot of actual versus predicted responses (a) thermal conductivity ratio (b) Zeta potential

Effect of Selected Factors on the Thermal Conductivity Ratio

Previous experimental studies showed well-dispersed metallic Nanofluids at low volume fractions in liquids, may enhance the mixture's thermal conductivity, k_{nf}, over the base-fluid values. The thermal conductivity enhancement of nanofluids depends on several mechanisms such as aggregation, Brownian motion, clustering of the nanoparticles and liquid layering around the nanoparticles [19]. Avoiding clustering effect by increasing temperature enhance the thermal conductivity [20]. Several significant factors such as temperature, particle volume fraction, pH of the nanofluid affects the thermal conductivity phenomena. 3D Graph and contour line map of the models for the thermal conductivity ratio of nanofluid are presented in Figures 7-9. Figure 7 demonstrates the variations in the thermal conductivity ratio in terms of the temperature and particle concentration variables while the solution pH was kept constant at the center point. By the response graph it is evident that increasing temperature consistently increases the thermal conductivity. This enhancement in thermal conductivity occurred due to Brownian movement increases with the increase of the nanofluid's bulk temperature. Therefore, these nano particles have an ability to transfer more energy from one place to another per time unit. Increase of particle volume fraction also increases the thermal conductivity ratio but it is limited to certain values to become nominal. Increasing particle volume fraction increases agglomeration. Hence to improve dispersion and reduce vanderwalls force, dispersing agents such as SDS were used. It was also evident that change in thermal conductivity with temperature and particle volume fraction was purely dependent on the pH value, as shown in Figures 8 and 9. The pH value strongly affects the electrostatic charge of the particle surface. Increasing pH increases thermal conductivity upto isoelectric point.

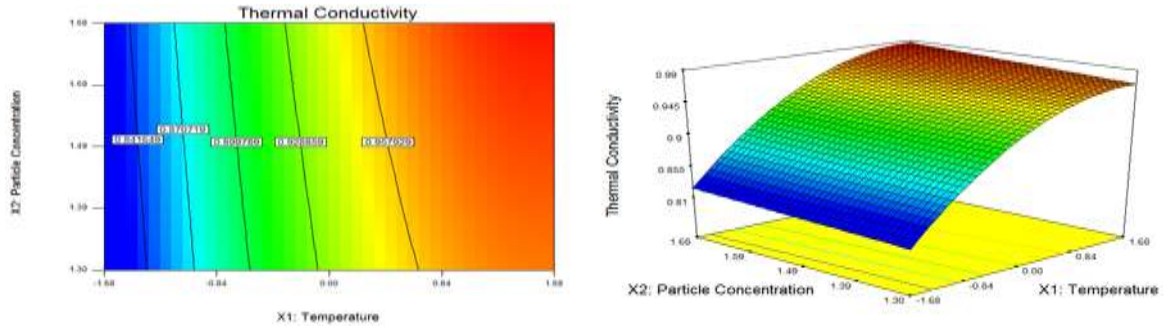

(a) (b)

Fig :7 Response surface and contour plots showing the mutual effect of temperature and particle concentration on thermal conductivity

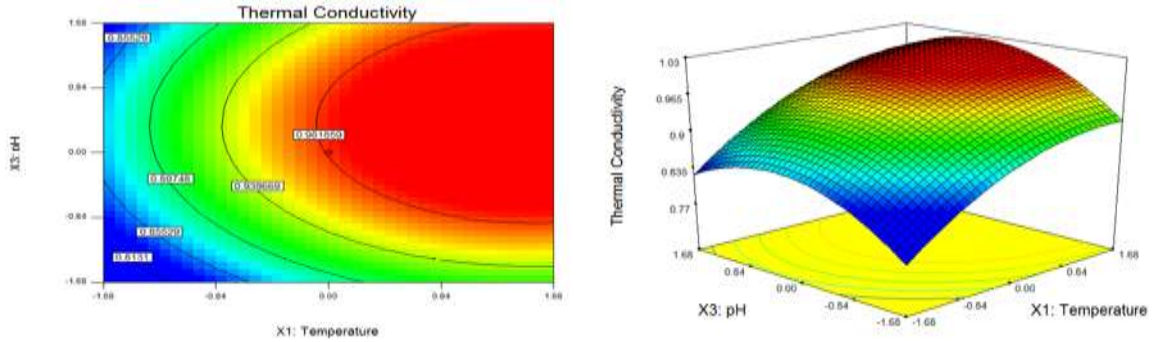

(a) (b)

Fig: 8 Response surface and contour plots showing the mutual effect of temperature and solution pH on thermal conductivity

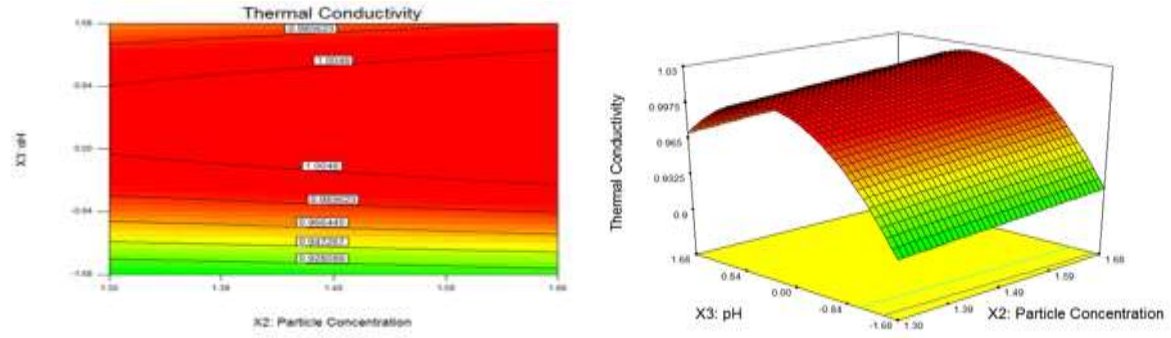

(a) (b)

Fig. 9. Response surface and contour plots showing the mutual effect of solution pH and particle concentration on thermal conductivity

Effect of Selected Factors on the Zeta Potential of the Nanofluid

The most important factor that affects zeta potential is pH. No flocculation occurs if all the particles in suspension have a large negative or positive zeta potential because they tend to repel each other. However, if the particles have low zeta potential values then there is no force to stop the particles approaching together and flocculating. The general dividing line between stable and unstable suspensions is generally taken at either +30mV or -30mV. Particles with zeta potentials more positive than +30mV or more negative than -30mV are normally considered stable. The major challenge in nanofluid systems is the rapid settling of the nanoparticles in fluids. The zeta potential decline is caused by several factors such as nanoparticle clustering, agglomeration and close packing of the dispersed phase. Thus, in order to obtain a better understanding of the results, the three dimensional (3D) response surface plots and contour lines map of the predicted models for zeta potential of the nanofluid are presented in Figures 10-12. The mutual effect of temperature and particle volume fraction at constant solution pH of 5 on stability (zeta potential) of mgO nanofluid is shown in Figure 5. The minimum zeta potential (maximum stability) for tin dioxide nanoparticles is observed at high levels of both selected factors. This minimum is equal to -22. It was observed that the zeta potential decreases (stability increased) upon increasing temperature and particle volume fraction. These facts should take into account that the temperature directly regulates particle kinetic energies, Brownian motion of nanoparticles and finally the coagulation efficiency. Therefore, if the kinetic

energy of the particles is lower than their interaction potential, coagulation of two particles occurs after collision. Also, the formation probability of bigger agglomerates increases at low temperatures [21]. It is clear from Figure 10 that the stability increases upon increasing mgO concentration. This conduct happened due to high viscosity of a nanofluid than base fluid and increases with an increase in the particle volume concentration. And also stability increases due to the high surface area and surface activity. Using better surfactant is important to enhance the stability of nanoparticles in the base fluid [22]. Surfactants play a very crucial role in nanofluid systems. The concentration of the surfactant has a positive effect on the dynamic viscosity of nanofluids and prevents the nanoparticle agglomeration due to the increase of electrostatic repulsion between the suspended particles. Consequently, adding surfactant significantly minimizes particle aggregation and enhances the dispersion behavior. The maximum response zone of stability is observed at pH values of 7 to 8.25 at each temperature level which is shown in figure 11. This illustrates that increasing the pH up to 7-8 will enhance stability. This behavior is due to the fact that the stability of a nanofluid is related to its electrokinetic properties. At the isoelectric point (IEP), the repulsive forces between mgO nanoparticles tend towards zero and nanoparticles will coagulate together at this pH value. The hydration forces between nanoparticles increase as the pH of the solution departs from the IEP, which results in the enhanced mobility of nanoparticles in the suspension and the colloidal particles become more stable (Habibzadeh et al., 2010; Goharshadi et al., 2013). At high and low levels of solution pH, stability has a tendency to decrease which is shown in figure 12. Theoretically, this may be attributed to the decrease of the surface charge. As a result, a weakly repulsive double layer force is generated.

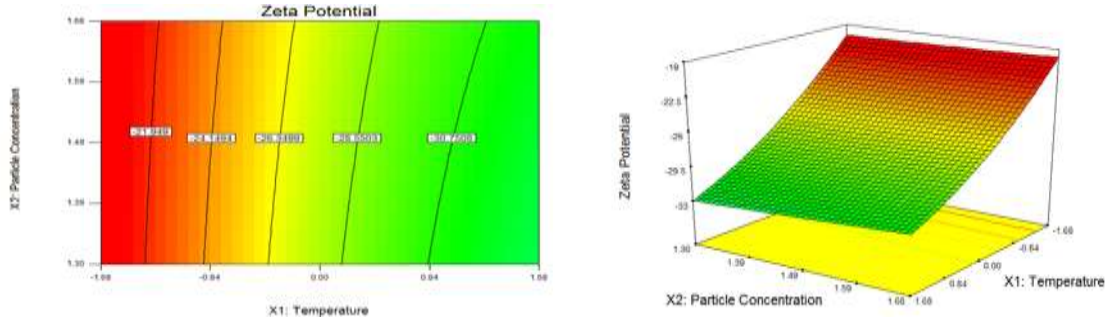

(a) (b)

Fig:10 Response surface and contour plots showing the mutual effect of temperature and particle concentration on Zeta Potential

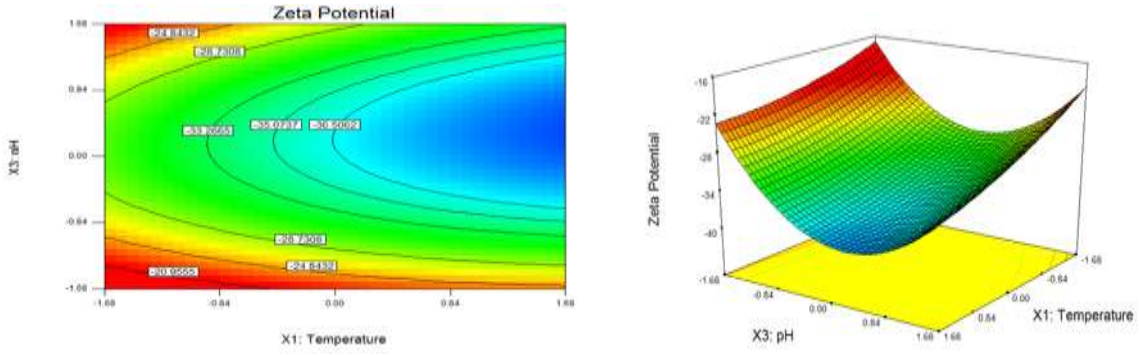

(a) (b)

Fig: 11. Response surface and contour plots showing the mutual effect of temperature and solution pH on Zeta Potential

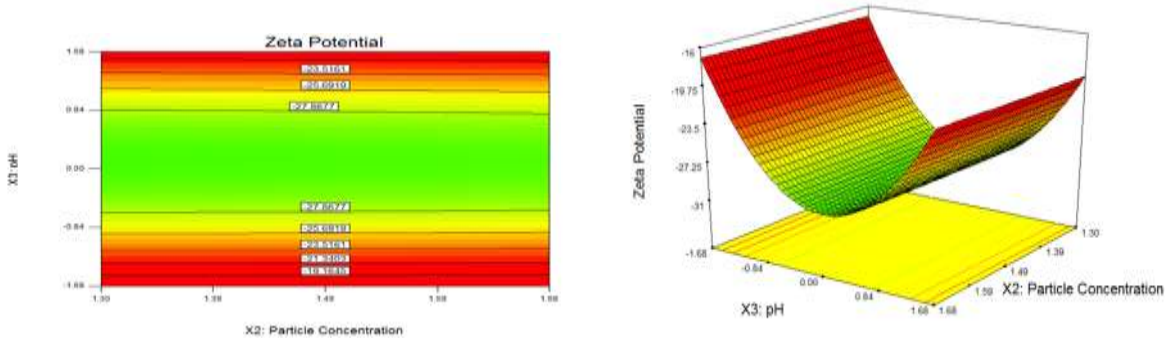

(a) (b)

Fig: 12. Response surface and contour plots showing the mutual effect of solution pH and particle concentration on Zeta Potential

CONCLUSION

The Performance of MgO nanofluid was experimented and predicted using CCRD design successfully to measure the optimum results for thermal conductivity and Zeta potential. The optimal experimental conditions based on the different coded factors and their corresponding responses were carried out by minimizing the zeta potential and maximizing thermal conductivity ratio which is shown in Table 7. The optimal process conditions determined by the CCRD method based on the actual values of the factors are as follows,

Table 7 Optimum Experimental Condition

Optimum Result	Factors			**Thermal Conductivity**	**Zeta Potential**	**Desirability**
	Temperature	**Particle Concentration**	**pH**			
1	48.69	3.73	9.05	0.99	----	1
2	32.09	3.13	5.15	----	-22	1

REFERENCES

1. K. Kaviyarasu and P. A. Devarajan, “A versatile route to synthesize MgO nanocrystals by combustion technique,” Der Pharma Chemica, vol. 3, no. 5, pp. 248–254, 2011.
2. S. Suresh and D. Arivuoli, “Synthesis and characterization of Pb + doped MgO nanocrystalline particles,” Digest Journal of Nanomaterials and Biostructures, vol. 6, no. 4, pp. 1597–1603, 2011.
3. B. Nagappa and G. T. Chandrappa, “Mesoporous nanocrys- talline magnesium oxide for environmental remediation,” Microporous and Mesoporous Materials, vol. 106, no. 1-3, pp. 212–218, 2007.
4. Saidur, R., Leong, K.Y. and Mohammad, H.A., A review on applications and challenges of nanofluids. Renewable and sustainable energy reviews, 15(2011), 3, pp.1646-1668.
5. Duangthongsuk, W. and Wongwises, S., Heat transfer enhancement and pressure drop characteristics of TiO_2–water nanofluid in a double-tube counter flow heat exchanger. International Journal of Heat and Mass Transfer, 52(2009), 7, pp.2059-2067.
6. Kayhani, M.H., Soltanzadeh, H., Heyhat, M.M., Nazari, M. and Kowsary, F., Experimental study of convective heat transfer and pressure drop of TiO 2/water nanofluid. International Communications in Heat and Mass Transfer, 39(2012), 3, pp.456-462.
7. Das, K., Slip flow and convective heat transfer of nanofluids over a permeable stretching surface. Computers & Fluids, 64 (2012), pp.34-42.
8. Pandiaraj, P., Gnanavelbabu, A. and Saravanan, P., Synthesis of CuO Nanofluids and Analysis of its increased effective thermal conductivity for Flat Plate Heat Pipe. International Journal of ChemTech Research, 8(2015), 4, pp.1972-1976.
9. Mahbubul, I.M., Saidur, R. and Amalina, M.A., Influence of particle concentration and temperature on thermal conductivity and viscosity of Al2O 3/R141b nanorefrigerant. International Communications in Heat and Mass Transfer, 43(2013), pp.100-104.
10. Esfe, M.H. and Saedodin, S., An experimental investigation and new correlation of viscosity of ZnO–EG nanofluid at various temperatures and different solid volume fractions. Experimental thermal and fluid science, 55(2014), pp.1-5.
11. Esfe, M.H., Saedodin, S. and Mahmoodi, M., Experimental studies on the convective heat transfer performance and thermophysical properties of MgO–water nanofluid under turbulent flow. Experimental thermal and fluid science, 52(2014) , pp.68-78
12. Kazemi-Beydokhti, A., Namaghi, H.A. and Heris, S.Z., 2013. Identification of the key variables on thermal conductivity of CuO nanofluid by a fractional factorial design approach. Numerical Heat Transfer, Part B: Fundamentals, 64(6), pp.480-495.
13. Gheshlaghi, R., et al. "Application of statistical design for the optimization of amino acid separation by reverse-phase HPLC." Analytical biochemistry 383.1 (2008): 93-102.
14. Akhtar, M., 2001. Five-factor central composite designs robust to a pair of missing observations. J. Res. Sci, 12(2), pp.105-115.
15. Habibzadeh, S., Kazemi-Beydokhti, A., Khodadadi, A.A., Mortazavi, Y., Omanovic, S. and Shariat-Niassar, M., 2010. Stability and thermal conductivity of nanofluids of tin dioxide synthesized via microwave-induced combustion route. Chemical Engineering Journal, 156(2), pp.471-478.
16. Nagasaka, Yuji, and A. Nagashima. "Absolute measurement of the thermal conductivity of electrically conducting liquids by the transient hot-wire method." Journal of Physics E: Scientific Instruments 14.12 (1981): 1435.

17. Evans, W., Prasher, R., Fish, J., Meakin, P., Phelan, P. and Keblinski, P., 2008. Effect of aggregation and interfacial thermal resistance on thermal conductivity of nanocomposites and colloidal nanofluids. International Journal of Heat and Mass Transfer, 51(5), pp.1431-1438.

18. Tucknott, R. and Yaliraki, S.N., 2002. Aggregation properties of carbon nanotubes at interfaces. Chemical physics, 281(2), pp.455-463.

19. Pirahmadian, M.H. and Ebrahimi, A., 2012. Theoretical Investigation heat transfer mechanisms in nanofluids and the effects of clustering on thermal conductivity. International Journal of Bioscience, Biochemistry and Bioinformatics, 2(2), p.90.

20. Das, S.K., Putra, N., Thiesen, P. and Roetzel, W., 2003. Temperature dependence of thermal conductivity enhancement for nanofluids. Journal of heat transfer, 125(4), pp.567-574.

21. Fiedler, S.L., Izvekov, S. and Violi, A., 2007. The effect of temperature on nanoparticle clustering. Carbon, 45(9), pp.1786-1794.

22. Yu, W. and Xie, H., 2012. A review on nanofluids: preparation, stability mechanisms, and applications. Journal of Nanomaterials, 2012, p.1.

Author' biography with Photo

P.Pandiyaraj received B.E., degree in Mechanical Engineering from Coimbatore institute of Technology, India and M.E., degree in Thermal Engineering from National Institute of Technology, Trichy India, in 1985 and 2006, respectively. Currently he is pursuing his Ph.D. degree in Anna University, India. His research areas are Flat plate heat pipes, Computational Fluid Dynamics, Heat exchangers design, nanofluids and optimization.

Dr.A.Gnanavelbabu received B.E., degree in Mechanical Engineering from University of Madras, India and M.Tech., degree in Industrial Engineering from National Institute of Technology,Trichy India. He Completed his Ph.D. in Industrial Engineering from Faculty of Mechanical Engineering, National Institute of Technology, Trichy. He is currently working as a Associate Professor, Department of Industrial Engineering in Anna University Chennai. His research areas are Tribology of advanced materials, Composites, Computational Intelligence, Lean Sigma, Supply Chain Management.

P.Saravanan received B.E., degree in Electronics and Communication Engineering from St.Joseph's College of Engineering and Technology, India and M.Tech., degree in Nanoscience and Technology from Anna University BIT Campus, Trichy, India. Currently he is pursuing his Ph.D. degree in Anna University, India. His research areas are thin film technology, semiconductor devices, nanofluids and optoelectronics.